THIS MONTH IN

JNM

Multipurpose microbubbles: Kiessling and colleagues offer an overview of ultrasound microbubble applications in preclinical and clinical molecular diagnosis, therapy, and a wide range of potential combinations of diagnostic and therapeutic agents and mechanisms. . . . . ***Page 345***

Viability and STICH: Perrone-Filardi and Pinto provide commentary on the results of a trial that has led to scrutiny of the role of myocardial viability and its assessment in treatment outcomes in patients with left ventricular dysfunction. . . . . ***Page 349***

PET and gallbladder polyps: Lee and colleagues determine the value of ^{18}F-FDG uptake in gallbladder polyps for risk stratification in surgical intervention and identify optimal cutoff parameters for PET differentiation of malignant from benign polyps. . . . . ***Page 353***

Evaluating thyroid cancer metastases: Van Nostrand and colleagues compare the results of 2 common methods of patient preparation for detection of metastases from differentiated thyroid cancer using ^{131}I whole-body imaging and ^{124}I PET. . . . . ***Page 359***

PET and progesterone receptors: Dehdashti and colleagues report on the safety and dosimetry of an ^{18}F-labeled progesterone analog and on the feasibility of PET imaging of tumor progesterone receptors in breast cancer. . . . . ***Page 363***

PET after radioembolization: Haug and colleagues evaluate ^{18}F-FDG PET/CT for predicting survival in patients undergoing ^{90}Y selective internal radiation therapy for unresectable, chemotherapy-refractory hepatic metastases from breast cancer. . . . . ***Page 371***

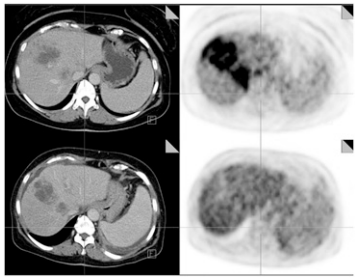

^{18}F-Florbetapir PET and amyloid: Joshi and colleagues examine the effective dose range and test–retest reliability of ^{18}F-florbetapir PET using visual assessment and quantitative values in patients with Alzheimer disease and cognitively normal individuals. . . . . ***Page 378***

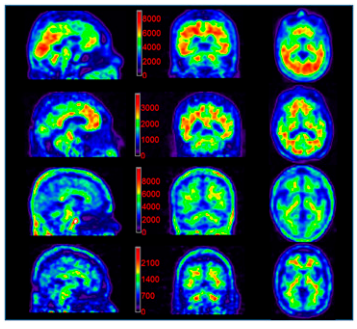

PET and NOP receptors: Lohith and colleagues assess the ability of a high-affinity PET ligand, ^{11}C-NOP-1A, to quantify nociceptin/orphanin FQ peptide receptors in healthy human brains. . . . . ***Page 385***

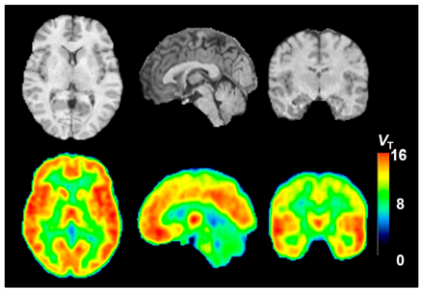

^{18}F-DOPA PET/CT and treatment: Walter and colleagues survey referring physicians to evaluate the impact of ^{18}F-DOPA PET/CT imaging on clinical management of patients with known or suspected brain tumors. . . . . ***Page 393***

DAT loss in atypical parkinsonism: Oh and colleagues use ^{18}F-FP-CIT PET to explore and identify differences in striatal subregional dopamine transporter loss in Parkinson disease, progressive supranuclear palsy, and multiple system atrophy. . . . . ***Page 399***

PET and hypertrophic cardiomyopathy: Bravo and colleagues look at PET parameters of microvascular function in groups of patients with obstructive and nonobstructive hypertrophic cardiomyopathy. . . . . ***Page 407***

^{18}F-AZD4694 PET: Cselényi and colleagues describe the results of clinical studies with this amyloid-β radioligand with high specific and low nonspecific binding in patients with Alzheimer disease and control subjects. . . . . ***Page 415***

PET and liver physiology: Keiding provides an educational overview of recent developments in dynamic PET for assessing liver physiology and biochemistry, including methods for direct quantification of regional blood perfusion, metabolic processes, and biliary excretory functions. . . . . ***Page 425***

^{18}F-L-FEHTP PET tumor imaging: Krämer and colleagues evaluate in vitro and in vivo characteristics of this tryptophan analog as a PET probe for endocrine and nonendocrine tumor imaging. . . . . ***Page 434***

Imaging EGFR TKI resistance: Zannetti and colleagues describe mouse studies

conducted to determine whether ^{18}F-FLT PET/CT can be useful in selection of patients with non–small cell lung cancer for treatment with epidermal growth factor receptor tyrosine kinase inhibitors. . . . . ***Page 443***

β-Glucuronidase in neuroinflammation: Antunes and colleagues investigate the ability of ^{18}F-FEAnGA PET to detect β-glucuronidase release during neuroinflammation in a rat model of herpes encephalitis. . . . . ***Page 451***

Sentinel node SPION SPECT/MRI: Madru and colleagues report on the development of a multimodal SPECT/MRI contrast agent using ^{99m}Tc-labeled superparamagnetic iron oxide nanoparticles for sentinel lymph node mapping in animal studies. . . . . ***Page 459***

Tumor vasculature imaging: Mees and colleagues describe the radiosynthesis and preclinical evaluation of a ^{99m}Tc-labeled tracer that specifically binds tumor subendothelial collagen and thereby facilitates imaging of tumor vasculature. . . . . ***Page 464***

^{18}F-pyridaben analogs for MPI: Mou and colleagues detail the synthesis, characterization, and initial evaluation of two ^{18}F-labeled pyridaben analogs as potential agents for PET myocardial perfusion imaging. . . . . ***Page 472***

Targeting Nuclisome particles: Gedda and colleagues present a 2-step targeting strategy to transport Auger-electron–emitting radionuclides into the cell nucleus by means of nuclide-filled liposomes and report on experiments in a small-animal study. . . . . ***Page 480***

Tumor selectivity of ^{11}C-4DST: Toyohara and colleague evaluate the tissue kinetics and biodistribution of ^{11}C-4DST in rodent tumor and acute sterile inflammation models and compare results with those of other more frequently used ligands. . . . . ***Page 488***

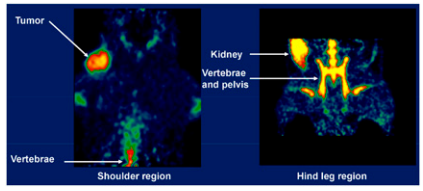

PET motion correction: Keller and colleagues describe the development of quality control methods for PET motion correction procedures based on external motion tracking for high-resolution human brain scanning. . . . . ***Page 495***

ON THE COVER

In this glioblastoma patient, the gadolinium-enhanced T1-weighted MR image showed irregular nodular enhancement suggestive of recurrent disease. Intense activity on ^{18}F-DOPA PET at the site of suspected recurrence increased the suspicion from moderate to high. Accordingly, patient management was changed from wait and watch to chemotherapy.

See page 396.